Soft Matter

PAPER

Cite this: *Soft Matter*, 2018, **14**, 6561

Effective Hamiltonian of topologically stabilized polymer states

K. Polovnikov, [ab] S. Nechaev*[cd] and M. V. Tamm[be]

Received 16th April 2018,
Accepted 18th July 2018

DOI: 10.1039/c8sm00785c

rsc.li/soft-matter-journal

Topologically stabilized polymer conformations in melts of nonconcatenated polymer rings and crumpled globules are considered to be a good candidate for the description of the spatial structure of mitotic chromosomes. Despite significant efforts, the microscopic Hamiltonian capable of describing such systems still remains unknown. We describe a polymer conformation by a Gaussian network – a system with a Hamiltonian quadratic in all coordinates – and show that by tuning interaction constants, one can obtain equilibrium conformations with any fractal dimension between 2 (an ideal polymer chain) and 3 (a crumpled globule). Monomer-to-monomer distances in topologically stabilized states, according to available numerical data, fit very well the Gaussian distribution, giving an additional argument in support of the quadratic Hamiltonian model. Mathematically, the polymer conformations are mapped onto the trajectories of a subdiffusive fractal Brownian particle. Moreover, we explicitly show that the quadratic Hamiltonian with a hierarchical set of coupling constants provides the microscopic background for the description of the path integral of the fractional Brownian motion with an algebraically decaying kernel.

I. Introduction

Classical statistical physics of polymers relies on the study of three archetypical polymer states: the ideal, swollen, and collapsed polymer chains.[1–4] Equilibrium conformational statistics of linear polymers can be described by combinations of these models for any concentrations and chain interaction parameters.

In ideal macromolecules the elementary units do not interact with each other apart from being sequentially connected. A statistical description of ideal chains is based on the analogy between the equilibrium ensemble of ideal polymer chain conformations and trajectories of Brownian particles: similarly to the ensemble of random walks, ideal linear polymers in a free space have Gaussian statistics with the fractal dimension $d_f = 2$. This analogy can be easily generalized to the case of ideal polymers in external potentials.

A swollen polymer state emerges due to the presence of excluded volume interactions, *i.e.* repulsion between monomer units, which are distant along the chain but close in space. The corresponding partition function can be interpreted as a self-avoiding random walk. The properties of swollen polymers are well understood due to the famous polymer-magnetic analogy proposed by de Gennes[5] for solitary chains and extended by Des Cloizeaux[6] to polymers in solutions. In particular, the statistics of swollen chains in two- and three-dimensional spaces is known to be non-Gaussian, though self-similar, with corresponding fractal dimensions being equal to 4/3 in 2D and approximately 1.7 in 3D.

Properties of collapsed polymer chains are governed by an interplay of attractive and repulsive interactions between monomer units. Implying existence of attractive interactions only, one arrives at an unphysical conclusion that a polymer collapses to a point. Stabilization of a polymer chain in the collapsed regime is due to the equilibration between two-body attractive and three-body repulsive interactions. In the mean-field approximation the statistics of the resulting states can be described in terms of an ideal chain in an external self-consistent field created by volume interactions among distant parts of the chain (or other chains in a multi-chain setting).[1,7,8]

It has become clear in recent years that these three classical archetypes do not exhaust the variety of macromolecular states existing in bio- and synthetic polymers. In particular, the statistics of ring polymers with fixed topology is definitely not covered by any of them. Contrary to linear polymers, rings preserve their topology: for example, initially nonconcatenated rings cannot get into a concatenated state without being ruptured. The resulting topological repulsion between nonconcatenated rings drastically changes the statistical properties of chains in a melt.[9–15] It has been conjectured in ref. 9 that conformations of long unknotted and non-concatenated ring polymers in melts are compact

[a] *Skolkovo Institute of Science and Technology, 143026 Skolkovo, Russia*
[b] *Faculty of Physics, Lomonosov Moscow State University, 119992 Moscow, Russia*
[c] *Interdisciplinary Scientific Center Poncelet (ISCP), 119002, Moscow, Russia. E-mail: sergei.nechaev@gmail.com*
[d] *Lebedev Physical Institute RAS, 119991, Moscow, Russia*
[e] *Department of Applied Mathematics, MIEM, National Research University Higher School of Economics, 101000, Moscow, Russia*

fractals with the fractal dimension $d_f = 3$ starting from some minimal scale, called entanglement length, N_e. This conjecture is now well-established both numerically (see, *e.g.* ref. 16 and 17) and in several competing semi-analytical theories.[11–14]

Contrary to ideal and swollen chains, the interactions in topologically stabilized globular polymers are substantially non-local. In a dense system, such as a collapsed ring, the topology is not screened and an explicit microscopic Hamiltonian for non-phantom rings is unknown. Development of the description of topologically interacting polymers based on first principles remains an open fundamental problem. The interest in topologically regulated polymer conformations is driven by experimental and numerical evidence that similar states may be observed as transient metastable conformations of linear polymers[18,19] relevant for understanding chromosome packing in living cells.[20,21] This conjecture is based on the estimates that the lifetime of such transient states may exceed the biologically relevant timescales[22] (see also ref. 17). As an alternative to this view, there have been recently proposed several other possible models explaining chromosome packing in living cells. Some of them involve the concept of reversible bridging between parts of the chromosomes[23] and non-equilibrium loop extrusion processes[24,25] and compactisation of chromosomes due to the absence of crowding agents.[26] All these models have a common feature: in a wide range of length scales, the resulting equilibrium chromatin packing is fractal with the fractal dimension d_f lying in the interval $2 \le d_f \le 3$. However, the microscopic Hamiltonian of these self-similar conformations is unknown, which sufficiently hardens the analytical tractability of corresponding theories.

In this paper we show that it is possible to design a Hamiltonian of pairwise interactions for polymer chains in such a way that the resulting polymer conformations in thermal equilibrium are fractal with prescribed fractal dimension $2 \le d_f \le 3$. The statistics of the resulting chain conformations is identical to the statistics of trajectories of a fractal Brownian motion (fBm).[27] From that perspective, our result is a generalization of the classical analogy between Brownian motion and ideal polymer chains.

The paper is organized as follows. In Section II we recall a mapping of polymer conformations onto particle trajectories. In Section III we construct the microscopic Hamiltonian that generates Gaussian polymer conformations and prove that such a description is identical to the theory of the fractal Brownian motion. In Section IV we generalize the memory-dependent action derived in ref. 30, and establish its connection with the action of a fBm particle and provide the microscopic background for this correspondence. In Section V we show that the simulation data from earlier works,[28,29] where topologically stabilized polymer states were simulated, are consistent with the Gaussian monomer-to-monomer distribution typical of the quadratic Hamiltonian introduced in this paper, which forces us believe that the proposed Hamiltonian is a good candidate for the phenomenological description of topologically stabilized polymeric states.

II. Fractional Brownian motion as a conformation of a polymer chain

Statistical properties of long ($N \gg 1$) polymer chains are insensitive to specific microscopic details of chain flexibility, which gives us the freedom to choose a particular microscopic model of a chain. Here we use a beads-on-string model of a polymer chain with pairwise interactions between the beads. The chain conformation is characterized by coordinates of all $N+1$ units, $\mathbf{X} = \{\mathbf{x}_0, \mathbf{x}_1, \ldots, \mathbf{x}_N\}$. The typical bead-to-bead distance is a fluctuating variable with the mean square b^2, so the total length of the chain is $L = Nb$. The potential energy $U(\mathbf{X})$ of volume interactions between the beads is assumed to be a sum of pairwise interactions $V(\mathbf{x}_n,\mathbf{x}_{n'})$. The partition function $P(\mathbf{x}_k,\mathbf{x}_m)$ of the chain with k-th and m-th beads fixed at $\mathbf{x}_k$ and $\mathbf{x}_m$, respectively, can be expressed in terms of the Euclidean Feynman path integral (the Wiener measure in the probabilistic language)[2] with the action:

$$P(\mathbf{x}_k,\mathbf{x}_m) = \int \mathcal{D}\{\mathbf{X}\} \mathrm{e}^{-S\{\mathbf{X}\}};$$
$$S = \frac{3}{2b^2}\sum_{n=0}^{N-1}(\mathbf{x}_{n+1}-\mathbf{x}_n)^2 + \sum_{n=0}^{N}\sum_{n'=n+2}^{N} V(\mathbf{x}_n,\mathbf{x}_{n'}), \quad (1)$$

where the integration is taken over all possible conformations, $\mathcal{D}\{\mathbf{X}\} = \prod_{n\neq k,m} \mathrm{d}\mathbf{x}_n$. Here and below we measure all energetic terms in the dimensionless units or equivalently $k_BT = 1$.

In the absence of volume interactions, the partition function (1) obeys the diffusion equation with $\mathbf{x} = \mathbf{x}_k - \mathbf{x}_m$ and $s = |k-m|$ playing the role of the coordinate and time, respectively. Therefore, the equilibrium distribution of the monomer-to-monomer distance is the same as for the standard Brownian motion:

$$P(\mathbf{x}_k,\mathbf{x}_m,s) = \left(\frac{3}{2\pi s b^2}\right)^{3/2} \exp\left(-\frac{3(\mathbf{x}_k-\mathbf{x}_m)^2}{2sb^2}\right). \quad (2)$$

The distribution (2) means that conformations of ideal polymer chains are fractals with $d_f = 2$ similarly to Brownian trajectories. Here we generalize this analogy to the case of arbitrary fractal dimension d_f. Namely, we ask whether it is possible to choose pairwise interactions $V(\mathbf{x}_n,\mathbf{x}_{n'})$ in (1) in such a way that the resulting equilibrium monomer-to-monomer distances would have a Gaussian distribution with some prescribed fractal dimension d_f:

$$P(\mathbf{x}_k,\mathbf{x}_m,s) = \left(\frac{3}{2\pi b^2 s^{2/d_f}}\right)^{3/2} \exp\left(-\frac{3(\mathbf{x}_k-\mathbf{x}_m)^2}{2b^2 s^{2/d_f}}\right) \quad (3)$$

The behavior dictated by (3) is typical for the fBm, B_H, with $H = 1/d_f$, a process whose increments are the integrals over increments of ordinary Brownian motion weighted with a non-local algebraic memory kernel.[27] This process is strongly non-Markovian in a sense that correlations of fBm increments (positive for $H > 1/2$ and negative for $H < 1/2$) decay as a power-law. However, fBm is a linear function of Brownian motion, and is Gaussian in the sense of (3). It is, therefore,

an example of a Gaussian process with a scale-free memory. Importantly, fBm has stationary and self-similar increments. This makes it a plausible candidate for the description of crumpled polymer conformations.

There are several ways of constructing a Langevin formalism, which generates a process with fBm statistics. However, if one adds a requirement that the resulting process should also respect the fluctuation–dissipation theorem, there is a preferred form, known as the fractional Langevin equation (fLe) in the overdamped limit:[32–34]

$$\xi_H \int_0^t \mathrm{d}\tau K(t-\tau)\frac{\mathrm{d}\mathbf{r}(\tau)}{\mathrm{d}\tau} = \mathbf{F}_H(t); \quad \langle \mathbf{F}_H(t_1)\mathbf{F}_H(t_2)\rangle = \xi_H K(t_1-t_2);$$
$$K(t_1-t_2) = \frac{2(1-H)(1-2H)}{|t_1-t_2|^{2H}}. \tag{4}$$

In this paper, we show that for long polymer chains ($N \gg 1$) a pairwise potential:

$$V(\mathbf{x}_k,\mathbf{x}_m) = a_{km}(\mathbf{x}_k - \mathbf{x}_m)^2 \tag{5}$$

can be used to construct polymer chains with fBm-like equilibrium distribution of the monomer-to-monomer distance (3) with any d_f lying in the interval $2 < d_\mathrm{f} < 3$ provided that coefficients a_{km} depend only on chemical distance between monomers $|k-m| = s$ and decay asymptotically at $s \gg 1$ as

$$a_s \sim cs^{-\gamma}; \gamma \in (2,3) \tag{6}$$

with $c > 0$. The resulting large-scale fractal dimension of conformational statistics is related to the decay exponent γ by

$$d_\mathrm{f} = \frac{2}{\gamma - 2} \tag{7}$$

If $\gamma > 3$, *i.e.* the coefficients in (5) decay faster than s^{-3}, the statistics of the corresponding polymer chain remains ideal at large scales and the monomer-to-monomer distance is given by (2). The value of $\gamma = 3$ is critical, giving rise to logarithmic corrections in (2).

Quadratic interactions in (5) can be interpreted as a set of harmonic springs of varying rigidity connecting each pair of monomers, as shown in Fig. 1. It makes sense, therefore, to incorporate the nearest-neighboring harmonic interactions (*i.e.*, the first term in the action (1)) into the definition of V, such that $a_{k,k+1} = 3/(2b^2)$. The potential of the form (5) has appeared previously in various contexts. In particular, the resulting Gaussian networks[35–37] with (m,k)-depending rigidities are often used for the description of 3D structures of proteins. In ref. 38 and 39 static and dynamic properties of marginally compact trees with various fractal architectures were considered. A related hierarchical variational approach for an account of volume interactions of swollen polymer chains was proposed in ref. 40. The potential of the form (5) has appeared for the first time in a dynamic context in the work[41] on the so-called "beta-model", a Rouse-like model of a polymer chain with a time relaxation spectrum of a certain specific form. In ref. 42 a similar model was used for studying dynamic properties of a crumpled globule in a viscoelastic environment.

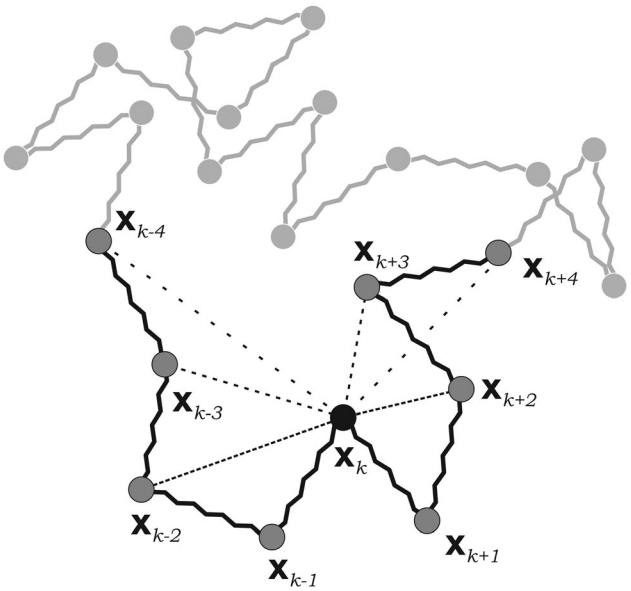

Fig. 1 Schematic image of the pairwise interactions (5) $V_{\mathbf{x}_k\mathbf{x}_m}$ of the k-th monomer ($\mathbf{x}_k$) with adjacent monomers of the chain with coordinates $\mathbf{x}_{k\pm1}$, $\mathbf{x}_{k\pm2}$, $\mathbf{x}_{k\pm3}$,.... Elastic constants a_{km} decay algebraically which is depicted by dashed lines with increasing spacing.

Using a harmonic potential (5), we propose an alternative form for the action of long fractional Brownian conformations, $N \to \infty$, which involves modification of the "kinetic" term in (1):

$$\tilde{P}(\mathbf{x},\mathbf{y}) = \int \mathcal{D}\{\mathbf{X}\}\mathrm{e}^{\tilde{S}}; \quad \tilde{S} = \int_0^\infty \mathrm{d}\xi \int_0^\infty \mathrm{d}\xi' \frac{\partial \mathbf{X}(\xi)}{\partial \xi}\frac{\partial \mathbf{X}(\xi')}{\partial \xi'}\varphi(|\xi-\xi'|) \tag{8}$$

where the function $\varphi(|\xi-\xi'|)$ is a power-law decaying memory kernel. Clearly, $\varphi(\xi) = \delta_\xi$ corresponds to a simple Brownian motion with $H = 1/2$. Action of the form (8) appeared previously in ref. 30, where it was shown that (8) with $\varphi(\xi) = \xi^{-1/2}$ corresponds to the statistics of trajectories of the Rouse particles, which is known to be fBm with $H = 1/4$. Here we generalize this result and show that for any $0 < H < 1/2$ the corresponding ensemble of fractal Brownian trajectories can be obtained from the action (8) with $\varphi(s) \sim s^{-2H}$.

III. Gaussian chain with long-range quadratic interactions

Here we prove the results outlined above, which connect the modes described by (5), and (6) with the fractal Brownian motion behavior (3). To simplify the description, take a ring chain of $N \gg 1$ monomers, $\mathbf{x}_N \equiv \mathbf{x}_0$. We consider phantom chains here, so for $|k-m| \ll N$ the distribution of $\mathbf{x}_k - \mathbf{x}_m$ does not depend on boundary conditions and this assumption does not lead to any loss of generality. Also, assume for definiteness that N is odd, $N = 2n+1$. The potential (5) in this case acquires the following form

$$V(\{\mathbf{X}\}) = \psi(\mathbf{x}_0,\mathbf{x}_1,\ldots,\mathbf{x}_{N-1}) = \sum_{m<k} a_s(\mathbf{x}_k - \mathbf{x}_m)^2 \tag{9}$$

where $s = s(k,m)$ is the shortest contour length between monomers k and m:

$$s(k,m) = \min(|k - m|, N - |k - m|) \tag{10}$$

This distance $s(k,m)$ is a symmetric and circularly periodic function

$$s(k,m) = s(m,k);\ s(k + i \mod N,\ m + i \mod N) = s(k,m) \tag{11}$$

It means that there are n independent different values of $a(s)$, $s = 1\ldots n$. Note that the standard ideal polymer ring corresponds to only nearest-neighbor interactions, $a(1) = 3/2b^2$ and $a(s) = 0$ for $s > 1$.

Introducing additionally

$$a(0) = 2\sum_{s>0} a(s) \tag{12}$$

one can rewrite potential (9)

$$V(\{\mathbf{X}\}) = \psi(\mathbf{x}_0, \mathbf{x}_1, \ldots, \mathbf{x}_{N-1}) = a(0)\sum_{m=0}^{N-1} x_m{}^2 - 2\sum_{m<k} a(s(k,m))\mathrm{x}_m\mathrm{x}_k = \langle X|\mathbb{A}|X\rangle \tag{13}$$

where matrix elements of $\mathbb{A}$ depend only on the distance between monomers $s(k,m)$. The structure of this matrix shares properties with a symmetric circulant matrix.[31] For example, for $n = 3$ and $N = 7$ the matrix $\mathbb{A}$ takes the form:

$$\mathbb{A} = -\begin{bmatrix} -a_0 & a_1 & a_2 & a_3 & a_3 & a_2 & a_1 \\ a_1 & -a_0 & a_1 & a_2 & a_3 & a_3 & a_2 \\ a_2 & a_1 & -a_0 & a_1 & a_2 & a_3 & a_3 \\ a_3 & a_2 & a_1 & -a_0 & a_1 & a_2 & a_3 \\ a_3 & a_3 & a_2 & a_1 & -a_0 & a_1 & a_2 \\ a_2 & a_3 & a_3 & a_2 & a_1 & -a_0 & a_1 \\ a_1 & a_2 & a_3 & a_3 & a_2 & a_1 & -a_0 \end{bmatrix}, \tag{14}$$

where, generally speaking, $a_{1,2,3}$ are arbitrary positive numbers, and a_0 is given by (12).

Eigenvectors of a circulant $\mathbf{A}_p$, $\mathbb{A}|\mathbf{A}_p\rangle = \omega_p|\mathbf{A}_p\rangle$ are known[31] to be

$$\mathbf{A}_p^{(k)} = \frac{1}{\sqrt{N}}\exp\left(\frac{2\pi ipk}{N}\right);\quad k = 0, 1\ldots N-1, \tag{15}$$

and the corresponding eigenvalues ω_p are

$$\omega_p = a(0) - \sum_{s=1}^{n} a(s)\left(\exp\left(\frac{2\pi ips}{N}\right) + \exp\left(\frac{2\pi ip(N-s)}{N}\right)\right) = 2\sum_{s=1}^{n} a(s)\left(1 - \cos\left(\frac{2\pi ps}{N}\right)\right). \tag{16}$$

Importantly, $\omega_0 = 0$ has the degeneracy 2, and other eigenvalues: $\omega_p = \omega_{N-p}$. Moreover, the spring constants $a(s)$ should decay faster than $1/s$ in order for expressions in (16) to converge. Physically, it means that strongly attractive elastic networks with slower decay of a_s get collapsed into a single point in the limit $N \to \infty$. In the Appendix A we consider a particular case of $a(s)$ decaying as a general power law $a(s) = cs^{-\gamma}$ and show (see (A6)) that in this case the eigenvalues with $p \ll N$ behave as

$$\omega_p \sim \begin{cases} \Gamma(1-\gamma)\left(\frac{p}{N}\right)^{\gamma-1} & \text{for } 2 < \gamma < 3 \\ \frac{1}{\gamma-3}\left(\frac{p}{N}\right)^2 & \text{for } \gamma > 3 \end{cases}, \tag{17}$$

where we keep only coefficients divergent at $\gamma \to 3$. Thus, for $\gamma > 3$ the interaction matrix has the usual Rouse spectrum (up to a γ-dependent prefactor) meaning that at equilibrium the chain is indistinguishable from an ideal chain (*i.e.*, a Gaussian chain with fractal dimension 2), and the existence of non-nearest neighbour interactions $a(s)$ for $s > 1$ simply renormalizes the chain persistence length. Meanwhile, if $2 > \gamma > 3$ a substantially different behavior arises.

The equilibrium properties of an elastic network are easier to analyze in terms of normal relaxation modes, $\mathbf{u}_p = \langle \mathbf{X}|\mathbf{A}_p\rangle$, $p = 0\ldots N-1$

$$\mathbf{u}_p = \frac{1}{\sqrt{N}}\sum_{k=0}^{N-1}\mathbf{x}_n\exp\left(\frac{2\pi ipk}{N}\right),\qquad \mathbf{x}_k = \frac{1}{\sqrt{N}}\sum_{p=0}^{N-1}\mathbf{u}_p\exp\left(-\frac{2\pi ipk}{N}\right) \tag{18}$$

In the new coordinates the potential (13) can be diagonalized, providing the following form

$$V(\{\mathbf{X}\}) = \sum_{m=0}^{N-1}\left\langle \mathbf{A}_m\middle|\mathbf{u}_m{}^*\sum_{p=0}^{N-1}\omega_p\mathbf{u}_p\middle|\mathbf{A}_p\right\rangle = \sum_{m=0}^{N-1}\sum_{p=0}^{N-1}\mathbf{u}_m{}^*\omega_p\mathbf{u}_p\langle\mathbf{A}_m|\mathbf{A}_p\rangle = \sum_{p=0}^{N-1}\omega_p|\mathbf{u}_p|^2 \tag{19}$$

where in the last equation we used that $\langle\mathbf{A}_m|\mathbf{A}_p\rangle = \delta_{m,p}$. In equilibrium, the distribution of energy between the addenda of (19) obeys the equipartition theorem, and therefore

$$\overline{\mathbf{u}_p{}^*\mathbf{u}_{p'}} = \frac{3\delta_{pp'}}{\omega_p} \tag{20}$$

where the bar denotes the equilibrium ensemble averaging.

Now, to prove that in the equilibrium the monomer-to-monomer distance $\mathbf{x}_k - \mathbf{x}_m$ for $1 \ll s(k,m) \ll N$ is given by the fBm distribution (3) we need to prove two statements: (i) that the equilibrium distribution is Gaussian, and (ii) that its variance grows as a power of s.

The statement (i) follows straightforwardly from the fact that the statistical weight of the full conformation $\mathbf{X} = \{\mathbf{x}_0,\ldots,\mathbf{x}_{N-1}\}$ is a Gaussian function:

$$P_N(\mathbf{X}) = \frac{1}{Z_N}\exp\{-\langle\mathbf{X}|\mathbb{A}|\mathbf{X}\rangle\}. \tag{21}$$

where Z_N is the partition function, and the Hamiltonian is given by (13). Since the Hamiltonian is translationally invariant, we get:

$$P(\mathbf{x}_k, \mathbf{x}_m, s) = \frac{1}{Z_N}\int \exp\{-\langle \mathbf{X}|\mathbb{A}|\mathbf{X}\rangle\} \prod_{i\neq k,m} \mathrm{d}\mathbf{x}_i = \left(\frac{3}{2\pi\sigma_{km}{}^2}\right)^{3/2} \exp\left(-\frac{(\mathbf{x}_k - \mathbf{x}_m)^2}{2\sigma_{km}{}^2}\right) \tag{22}$$

where the variance $\sigma_{km}{}^2 = \overline{(\mathbf{x}_k - \mathbf{x}_m)^2} \equiv \sigma^2(s)$, which is some function of the contour length $s(k,m)$. Rewriting this variance in terms of the normal modes (18) one gets:

$$\sigma^2(s) = \frac{1}{N}\overline{\left|\sum_{p=0}^{N-1} \mathbf{u}_p \left(\mathrm{e}^{\frac{-2\pi i p k}{N}} - \mathrm{e}^{\frac{-2\pi i p m}{N}}\right)\right|^2} = \frac{12}{N}\sum_{p=1}^{n} \omega_p{}^{-1}\left(1 - \cos\left(\frac{2\pi p s(k,m)}{N}\right)\right), \tag{23}$$

In (23) we used the degeneracy of the spectrum and the equipartition theorem (20).

To prove the statement (ii), note that the asymptotic behavior of (23) for $s \gg 1$ is controlled by the behavior of ω_p for $p \ll N$ and the typical relevant p is of order N/s. Therefore, to have algebraically decaying coefficients $a(s)$, one can use the expression (17), which gives

$$\sigma^2(s) \sim \frac{1}{N}\sum_{p=1}^{n} \left(\frac{p}{N}\right)^{1-\bar{\gamma}}\left(1 - \cos\left(\frac{2\pi p s(k,m)}{N}\right)\right) \sim \int_0^{\pi} x^{1-\bar{\gamma}}(1 - \cos xs)\mathrm{d}x = s^{\bar{\gamma}-2}\int_0^{\pi s} y^{1-\bar{\gamma}}(1 - \cos y)\mathrm{d}y, \tag{24}$$

where we used the notation

$$\bar{\gamma} = \begin{cases} \gamma & \text{for } 2 < \gamma < 3 \\ 3 & \text{for } \gamma > 3 \end{cases} \tag{25}$$

The integral on the right hand side converges for all relevant $\bar{\gamma}$ and for $s \gg 1$ only weakly depends on its upper limit, which allows us to extract the leading asymptotic

$$\sigma_s{}^2 \sim \begin{cases} s^{\bar{\gamma}-2} & \text{for } 2 < \gamma < 3 \\ s & \text{for } \gamma > 3 \end{cases} \tag{26}$$

Thus, if $a(s)$ decays slower than s^{-3}, the equilibrium conformations have fractal dimension $d_f = 2/(\gamma - 2)$, while for faster decays of $a(s)$ the chain adopts an ideal conformation akin to the standard Brownian trajectory, and the presence of additional terms in the potential (additional harmonic springs between beads) just renormalizes the chain stiffness. The equilibrium conformation of a chain is, therefore, an fBm with the Hurst exponent

$$H = \frac{\bar{\gamma}}{2} - 1 = \begin{cases} \gamma/2 - 1 & \text{for } 2 < \gamma < 3 \\ 1/2 & \text{for } \gamma > 3 \end{cases} \tag{27}$$

This result is, so far, obtained just for the case when the coefficients $a(s)$ decay strictly as a power law. In order to address a general situation, we evaluated (16) and (23) numerically for several specific choices of $a(s)$, in particular, of the form

$$a(s) = \begin{cases} c_1 s^{-\gamma_1} & \text{for } s < s^* \\ c_2 s^{-\gamma_2}, & \text{for } s > s^* \end{cases}, \tag{28}$$

The corresponding behavior is shown in Fig. 2. We see that in this case the chain as a whole is not a fractal anymore. Separation of scales is clearly seen: for $s \ll s^*$ the behavior of σ^2 is controlled by the exponent γ_1 while for $s \gg s^*$ it is controlled by γ_2. This means not only that the large-scale behavior of σ^2 depends only on the large-scale behavior of $a(s)$ in agreement with (26), but also that one can use the Hamiltonian (13) to construct polymer conformations with different fractal dimensions on different length scales and/or for different parts of the chain. This might be useful, *e.g.*, for the description of heterochromatin consisting of active and inactive domains (see *e.g.*, ref. 43–45).

The interpretation of a fBm trajectory as a specific type of polymer conformation suggests a natural way to determine the power spectrum $f(p)$ of the fBm. From the point of view of the polymer analogy $f(p)$ is related to the energy stored in the p-th normal mode, so equipartition theorem connects it with the eigenvalues ω_p of the interaction matrix $\mathbb{A}$:

$$f(p) = \overline{\mathbf{u}_p{}^*\mathbf{u}_p} \sim \omega_p{}^{-1}. \tag{29}$$

Taking into account (17) and (27) one gets

$$f(p) \sim \left(\frac{N}{p}\right)^{2H+1}. \tag{30}$$

which is a known result for the fBm.[46] Interestingly, within the Rouse approach to polymer dynamics, which corresponds to postulating

$$\frac{\partial \mathbf{x}_i}{\partial t} = \frac{\partial V(\mathbf{X})}{\partial \mathbf{x}_i} + \delta\text{-correlated Gaussian noise} \tag{31}$$

as equations of motion for individual monomers, $f(p)$ is also proportional to the relaxation time τ_p of the p-th mode.[29,42]

IV. Unifying action for fractional Brownian motion

In this section we discuss how naturally one can reinterpret the quadratic Gaussian interactions with algebraically decaying coefficients in terms of an action with a memory-dependent kernel as suggested by (8). The partition function of a polymer chain with quadratic interactions (13) reads as

$$Z_N = \int \mathcal{D}\{\mathbf{X}\}\mathrm{e}^{-S}; \quad S = \langle \mathbf{X}|\mathbb{A}|\mathbf{X}\rangle, \tag{32}$$

where integration is taken over $\mathcal{D}\{\mathbf{X}\} = \prod_{k=0}^{N} \mathrm{d}\mathbf{x}_k$ and S is the Euclidean action of a moving particle $\tilde{S}$.

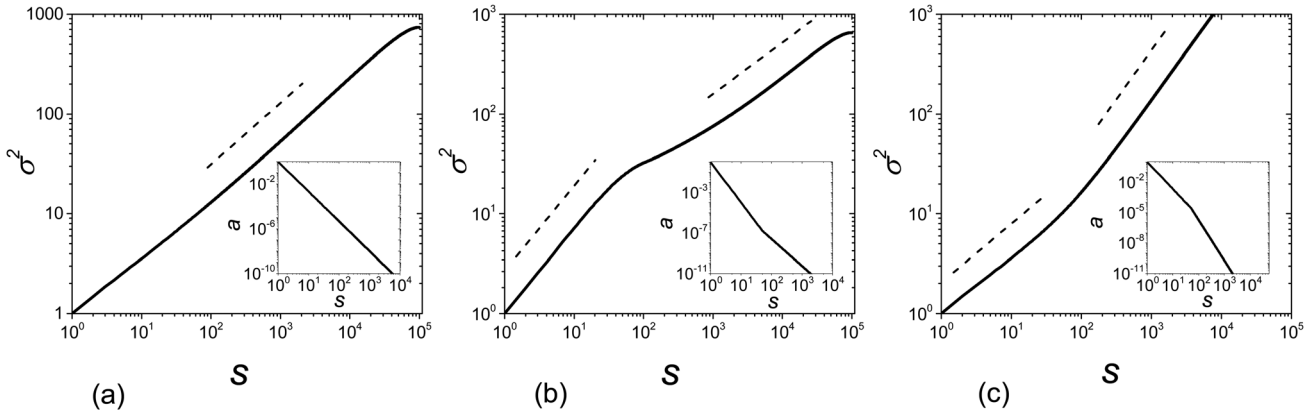

Fig. 2 Behavior of the dispersion $\sigma^2(s)$, $s = 1,\ldots,n$ defined in (23) for a ring chain with $n = 10^5$ for three cases: (a) single power-low decay $a(s) = s^{-8/3}$; (b and c) combination of two power laws (28) (b): $\gamma_1 = 4$, $\gamma_2 = 8/3$, $s^* = 100$, (c): $\gamma_1 = 8/3$, $\gamma_2 = 4$, $s^* = 100$. Dash lines correspond to $\sigma^2(s) \sim s^{2/3}$ (short dashes) and $\sigma^2(s) \sim s$ (long dashes). The plots are rescaled so that $\sigma^2(s) = 1$ for $s = 1$.

Discretizing the memory-dependent action in (8), one can write:

$$\begin{aligned}\tilde{S} &= \int_0^N \mathrm{d}\xi \int_0^N \mathrm{d}\xi' \frac{\partial \mathbf{X}(\xi)}{\partial \xi}\frac{\partial \mathbf{X}(\xi')}{\partial \xi'}\varphi(|\xi-\xi'|) \\ &\approx \sum_{k,m}^{N} (\mathbf{x}_k - \mathbf{x}_{k-1})(\mathbf{x}_m - \mathbf{x}_{m-1})\varphi_{k,m} \\ &= \sum_{k,m}^{N} \left(\varphi_{k,m} - \varphi_{k,m+1} - \varphi_{k+1,m} + \varphi_{k+1,m+1}\right)\mathbf{x}_k\mathbf{x}_m\end{aligned} \tag{33}$$

We see that indeed the two expressions (21) and (33) are equal provided that

$$a_{km} = -(\varphi_{k,m} - \varphi_{k,m+1} - \varphi_{k+1,m} + \varphi_{k+1,m+1}) \tag{34}$$

for all k, m. For $1 \ll |k-m| < n$ this reduces to

$$a(s = |k-m|) = (\varphi(s-1) + \varphi(s+1) - 2\varphi(s)) \simeq \frac{\partial^2 \varphi(s)}{\partial s^2} \tag{35}$$

As we have shown in the main text, the large-scale statistics of the chain depends only on the asymptotic behavior of $a(s)$. Thus, it is insensitive to particular details of the behavior of $a(s)$ or $\varphi(s)$ at small s. Assuming that for $s \to \infty$

$$a(s) \sim s^{-\gamma},\ \gamma \in (2,3), \tag{36}$$

one can approximate the difference in (35) by the continuous derivative. Thus, we arrive at the conclusion that (36) is equivalent to

$$\varphi(s) \simeq \frac{s^{2-\gamma}}{(\gamma-2)(\gamma-1)}, \quad \gamma \in (2,3) \tag{37}$$

Thus, we have shown that (32) can be rewritten as the action of a moving particle with the algebraically decaying memory kernel

$$\tilde{S} = \frac{1}{2H(2H+1)}\int_0^N \mathrm{d}\xi \int_0^N \mathrm{d}\xi' \frac{\partial \mathbf{X}(\xi)}{\partial \xi}\frac{\partial \mathbf{X}(\xi')}{\partial \xi'}\varphi(|\xi-\xi'|); \quad \varphi(s) \simeq \frac{1}{s^{2H}} \tag{38}$$

We see that the action of the form (38) with $\varphi(s)$ decaying as s^{-2H} for large s, where $H \in (0,1/2)$, generates an equilibrium ensemble of trajectories which is asymptotically equivalent to the fractional Brownian motion with the Hurst exponent H. In particular, for $H = 1/4$ we recover the action generating trajectories of beads of the Rouse chain,[30] while the case $H = 1/3$ corresponds to the Hurst exponent of the crumpled globule. For $H = 1/2$ algebraic representation is not valid and the kernel collapses $\varphi(s) \simeq \delta(s)$, recovering the kinetic action for ordinary Brownian motion.

Interestingly, it is possible to link the discussed representation of the fBm action with the fractional Langevin equation (fLe) (4) using a fluctuation–dissipation argument. The left-hand side of (4) corresponds to a dissipative friction force $\mathbf{F}$ acting on a fLe particle. At equilibrium, the average energy of the particle is conserved and the work performed by this force should be equal to the integral of the action $\tilde{S}$ along the trajectory of the particle. For a particle moving from $\mathbf{x}_1$ to $\mathbf{x}_2$ during the time t, the expression (38) adopts the form:

$$\tilde{S} = 2\int_0^t \mathrm{d}t' \int_0^{t'} \mathrm{d}t'' \frac{\partial \mathbf{x}(t')}{\partial t'}\frac{\partial \mathbf{x}(t'')}{\partial t''}\varphi(t'-t'') = -\int_{\mathbf{x}_1}^{\mathbf{x}_2} \mathbf{F}\mathrm{d}\mathbf{x} \tag{39}$$

Differentiating (39), one gets the following expression for the force $\mathbf{F}$:

$$\mathbf{F}(t) = -\int_0^t \mathrm{d}t' K_\alpha(t-t')\frac{\partial \mathbf{x}(t')}{\partial t'}; \quad K_\alpha(t-t') \sim \frac{1}{|t-t'|^{2H}}, \tag{40}$$

which, up to the choice of numerical coefficients, is identical to the one on the right hand side of (4).

Thus, the analogy between conformation of a polymer chain and trajectory of a subdiffusive fBm particle allows describing the latter in terms of an action that implies velocity–velocity correlations with an algebraically decaying memory kernel and provides the microscopic model behind the path integrals of moving particles with algebraic correlations. This action can be used to calculate the work performed by the friction force along the trajectory dictated by the fractional Langevin equation. Note that in equilibrium the energy loss due to friction is

compensated on average by the action of fractional noise in the thermostat, which in the formalism presented here emerges from the summation over "ghost" interactions between the particle velocity at a given point and velocities in all its future positions.

V. Discussion

In this paper we have shown that a polymer chain described by the Hamiltonian of the form (13) with coefficients decaying algebraically at large separation distances $a_{km} \sim |k-m|^{-\gamma}$ for $|k-m| \gg 1$ adopts a fractal Gaussian conformation with monomer-to-monomer distances growing as $|k-m|^{1/2}$ for $\gamma > 3$ and as $|k-m|^{(\gamma-2)/2}$ for $\gamma \in (2,3)$. Putting it in other terms, this means that adjusting parameters in (13) one can construct fractal *Gaussian* polymer conformations with any fractal dimension $d_f \geq 2$.

How physically relevant is this result? Can one, for example, use this Hamiltonian to describe topologically stabilized polymer states? The answer depends, to a large extent, on whether these polymer states, like nonconcatenated rings in a melt and mitotic chromosomes, are Gaussian or not. If they are, the potential (13) seems to be a good phenomenological Hamiltonian for such systems in the absence of an exact microscopic one, while if they are not, it can only be used to reproduce those properties of real chains which depend on the fractal dimension only.

To check whether the distributions obtained in numeric simulations of topologically stabilized polymer states are Gaussian or not, we used the available numerical data from two independent sources: the conformations of a long unknotted ring in a box with reflecting boundary conditions studied in ref. 28, and those of partially equilibrated crumpled globule conformations of linear chains with periodic boundary conditions generated in ref. 29. We plotted in Fig. 3 the distributions of monomer-to-monomer distance $\mathbf{x} \equiv |\mathbf{x}_k - \mathbf{x}_m|$ for different values of $s = |k-m|$ taken from the simulation data, and their best fit by the Maxwell distributions

$$P(\mathbf{x}) = 4\pi\mathbf{x}^2\left(\frac{3}{2\pi\sigma^2(s)}\right)^{3/2}\exp\left(-\frac{3\mathbf{x}^2}{2\sigma^2(s)}\right) \qquad (41)$$

Notably, a similar analysis was undertaken in ref. 47 where melts of much shorter (up to $N = 500$) poly(ethylene oxide) rings have been studied by molecular dynamics simulations (see Fig. 10 of ref. 47 for comparison). In all cases one can notice some visible discrepancies between numerical data and Maxwell distribution fit for small s, which can be attributed to unscreened excluded volume interactions and finite chain flexibility in the numerical experiments. Indeed, one expects similar behavior for linear chains where screening of volume interactions occurs at some finite concentration-dependent length scale of the order of the chain persistence length.

Meanwhile, for larger values of s the fits in Fig. 3a and b, as well as those in Fig. 10 of ref. 47 and 56, are remarkably good. Most importantly, they remain equally good for s larger than entanglement length N_e where the behavior of rings and crumpled globules is no longer described by the Flory theorem,[7] which can be seen by deviation of $\sigma^2(s)$ dependences from $\sigma^2(s) \sim s$, as shown in Fig. 3c and d. We find that the Maxwell curves fit the data of ref. 28 and 29 very well up to $s \approx N^{2/3}$, where the finite size effects become important.

We conclude, therefore, that the simple quadratic Hamiltonian (13) with coefficients calibrated to match experimentally observed

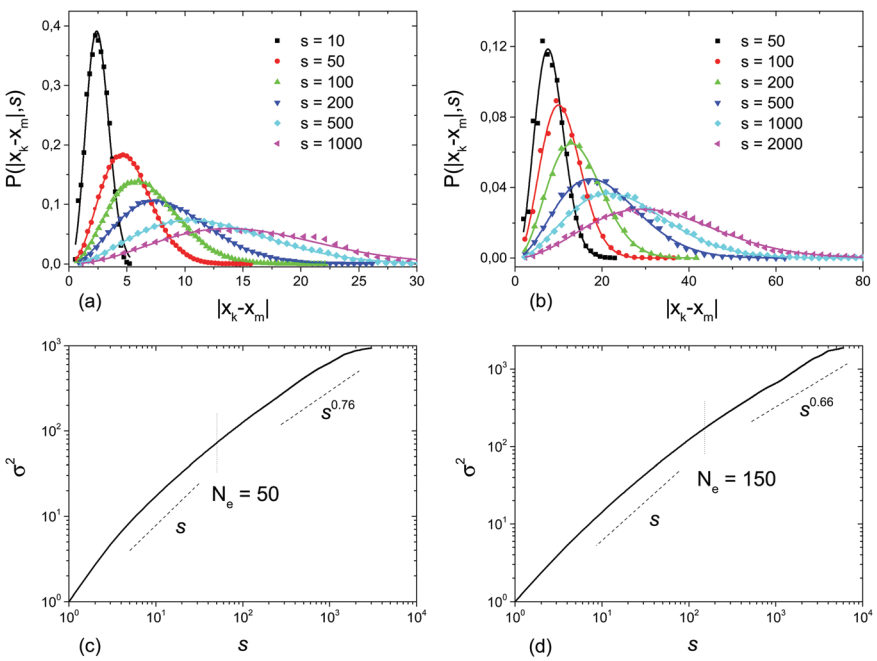

Fig. 3 (a and b) Distribution of the monomer-to-monomer distance $P(|\mathbf{x}_k - \mathbf{x}_m|,s)$ for different s for (a) partially equilibrated unknotted linear chains simulated in ref. 29 and (b) equilibrium unknotted rings in a box simulated in ref. 28 (points) together with their best fits with Maxwell distribution (41) (lines). (c and d) Variances of the best fit Maxwell distributions as functions of s, (c) data from ref. 29, $N_e \approx 50$, (d) data from ref. 28, $N_e \approx 150$.

fractal dimensions seems to be a very good candidate for an effective phenomenological description of topologically stabilized states. Indeed, within this formalism it should be possible to calculate various conformational characteristics of these states, including gyration radius, asphericity parameters, return probability, elastic properties, *etc.*, and there is even some hope that more complicated characteristics like knot invariants and surface exponents for $d_f = 3$ might be tractable. Hopefully, further research will shed more light on which of the properties of experimental systems can be reproduced exactly, and which need a consideration going beyond the phenomenological Hamiltonian suggested here.

In conclusion, consider briefly the dynamics of fractal polymer states with a fractal dimension different from 2. Detailed discussion of this topic goes beyond the scope of this paper, but let us mention that there exist two broad approaches. One is to develop a direct generalization of the Rouse model of polymer dynamics in a simple[2–4] or viscoelastic[50,51] medium for the $d_f \neq 2$ case. The resulting dynamics is characterized by monomer displacement at intermediate times scaling as[29,42,49]

$$\left\langle x_n^2(t) - x_n^2(0)\right\rangle \sim t^{2z}; \quad z = \frac{2\alpha}{2+d_f}, \tag{42}$$

where α is the dynamical exponent characterizing the surrounding medium, $\alpha = 1$ for a simple medium, and $\alpha < 1$ for the viscoelastic one. Importantly, for the case of $d_f = 3$, $\alpha = 1$ (42) is in reasonable agreement with computer simulations of a partially equilibrated system emulating the crumpled globule model of a chromosome[29] and is reproducing the dynamical exponent $z = 0.4$ for the chromosome loci of *E. coli* observed at timescales from 0.1 to 10 s.[52] Available single-particle tracking data for eukaryotic living-cells vary but typically give a somewhat smaller exponent, which might be explained within this approach by the viscoelasticity of nucleoplasm due to protein crowding. The Hamiltonian suggested above can be used to go beyond scaling considerations for the dynamics of these systems in the spirit of ref. 41 and 42. Indeed, within this approach, the generalized Rouse equation for the dynamics of the i-th bead takes the form

$$\xi\frac{\mathrm{d}\mathbf{x}_i(t)}{\mathrm{d}t} = \mathbf{f}_i(t) - \nabla_i H(\mathbf{X}); \quad \langle \mathbf{f}_i(t)\mathbf{f}_{i'}(t')\rangle = 6\xi\delta(t-t')\delta_{i,i'}, \tag{43}$$

where ∇_i denotes the gradient over $\mathbf{x}_i$, $\mathbf{f}_i$ is the stochastic thermal force, and $H(\mathbf{X})$ is given by (13). Further generalization in the case of the viscoelastic medium is also straightforward, see ref. 42 and 49.

On the other hand, the very applicability of the Rouse-like approach to, *e.g.*, melts of rings is questionable. Indeed, the presence of threading events slows down the dynamics[53–55] and seems to dictate the need for some generalization of the reptation model of polymer dynamics[2–4] to properly describe the observed phenomena. Such generalizations, suggested in ref. 13 and 14, give rise to values of $z \approx 0.26\ldots0.28$, which are much smaller than those predicted by Rouse-like theory. Numerical simulations of the dynamics of fully equilibrated ring melts of rings with N up to 500[47] and 1500[48] give rise to the effective dynamic exponent which is in between the two predictions. However, note that an underlying mechanism of classical polymer dynamics is the Rouse motion of the chain along the reptation tube. If similar Rouse-like movements in constrained geometry turn out to be important for the ring melts as well, the modified Rouse model with Hamiltonian-dependent force described as suggested by (43) may still be relevant.

Conflicts of interest

There are no conflicts to declare.

Appendix A: spectrum of the interaction matrix

Consider a chain with Hamiltonian (13) and coefficients behaving as $a(s) = cs^{-\gamma}$. Here we analyze the spectrum (16) of the matrix $\mathbf{A}$ for the physical range of exponents, $\gamma > 2$. In the continuum limit one has:

$$\begin{aligned}\omega_p &= 2^\gamma c\left(\frac{N}{\pi p}\right)^{1-\gamma}\int_{2\pi p/N}^{\pi p} x^{-\gamma}(1-\cos(x))\mathrm{d}x \\ &\approx 2^\gamma c\left(\frac{N}{\pi p}\right)^{1-\gamma}\left\{I(\gamma, p/N) - o\left(p^{1-\gamma}\right)\right\}\end{aligned} \tag{A1}$$

where the integral I is

$$\begin{aligned}I(\gamma, p/N) &= \int_{2\pi p/N}^{\infty} x^{-\gamma}(1-\cos(x))\mathrm{d}x \\ &= \frac{1}{\gamma-1}\left(\frac{2\pi p}{N}\right)^{1-\gamma} - \Re\left[i^{\gamma-1}\Gamma\left(1-\gamma, \frac{2\pi p i}{N}\right)\right]\end{aligned} \tag{A2}$$

and Γ is the holomorphic continuation of the upper incomplete Γ-function:

$$\begin{aligned}\Gamma(s,z) &= \Gamma(s) - \Gamma(s)z^s\exp(-z)\sum_{k=0}^{\infty}\frac{z^k}{\Gamma(s+k+1)} \\ &= \Gamma(s) - \frac{1}{s}z^s + \frac{1}{s+1}z^{s+1} - \frac{1}{s+2}z^{s+2} + o\left(z^{s+2}\right)\end{aligned} \tag{A3}$$

Using series (A3) one can rewrite the real part in (A2) as follows:

$$\begin{aligned}\Re\left[i^{\gamma-1}\Gamma\left(1-\gamma, \frac{2\pi p i}{N}\right)\right] &= \Gamma(1-\gamma)\cos\frac{\pi(\gamma-1)}{2} + \frac{1}{\gamma-1}\left(\frac{N}{2\pi p}\right)^{\gamma-1} \\ &\quad + \frac{1}{3-\gamma}\left(\frac{2\pi p}{N}\right)^{3-\gamma} + o\left(\left(\frac{\pi p}{N}\right)^{4-\gamma}\right)\end{aligned} \tag{A4}$$

Collecting (A4) and (A2), one ends up with the spectrum

$$\frac{\omega_p}{c} = -2^\gamma\left(\frac{\pi p}{N}\right)^{\gamma-1}\Gamma(1-\gamma)\cos\frac{\pi(\gamma-1)}{2} - \frac{8}{3-\gamma}\left(\frac{\pi p}{N}\right)^2 + o\left(\left(\frac{\pi p}{N}\right)^3\right) \tag{A5}$$

which yields the following asymptotic expression in the limit $p/N \to 0$:

$$\omega_p \sim \begin{cases} 2^\gamma \Gamma(1-\gamma)\cos\dfrac{\pi(3-\gamma)}{2}\left(\dfrac{\pi p}{N}\right)^{\gamma-1} & \text{for } 2<\gamma<3 \\ \dfrac{8}{\gamma-3}\left(\dfrac{\pi p}{N}\right)^2 & \text{for } \gamma>3 \end{cases} \quad \text{(A6)}$$

Acknowledgements

We are very grateful to M. Imakaev and A. Gavrilov who kindly provided us with the raw simulation data from ref. 28 and 29, respectively, to D. Grebenkov, R. Metzler, and G. Oshanin for numerous illuminating discussions and to A. Yu. Grosberg for critical comments on the manuscript. This work was supported by the EU-FP7-PEOPLE-IRSES grant DIONICOS (612707). SN gratefully acknowledges the RFBR grant 16-02-00252A for partial support; KP and MT acknowledge the support of the Foundation for the Support of Theoretical Physics and Mathematics ''BASIS'' (grant 17-12-278). A significant part of the work presented here was done during KP and MT visits to LPTMS at Universite Paris Sud, KP visits to the Theoretical Physics group at Potsdam University, and MT visits to Applied Mathematics Research Center at Coventry University. We use this opportunity to thank the hosts for their warm hospitality.

References

1 P.-G. de Gennes, *Scaling Concepts in Polymer Physics*, Cornell University Press, 1979.
2 M. Doi and S. F. Edwards, *The Theory of Polymer Dynamics*, Oxford University Press, Oxford, 1986.
3 A. Y. Grosberg and A. R. Khokhlov, *Statistical Physics of Macromolecules*, AIP Press, Woodbury, NY, 1994.
4 M. Rubinstein and R. Colby, *Polymer Physics*, Oxford University Press, Oxford, 2003.
5 P.-G. de Gennes, Exponents for the excluded volume problem as derived by the Wilson method, *Phys. Lett. A*, 1972, **38**, 339.
6 J. des Cloizeaux, The Lagrangian theory of polymer solutions at intermediate concentrations, *J. Phys.*, 1975, **36**, 281.
7 P. J. Flory, *Principles of Polymer Chemistry*, Cornell University Press, 1953.
8 I. M. Lifshitz, A. Y. Grosberg and A. R. Khokhlov, Some problems of the statistical physics of polymer chains with volume interaction, *Rev. Mod. Phys.*, 1977, **50**, 683.
9 A. R. Khokhlov and S. K. Nechaev, Polymer chain in an array of obstacles, *Phys. Rev. A: At., Mol., Opt. Phys.*, 1985, **112**, 156.
10 M. E. Cates and J. M. Deutsch, Conjectures on the statistics of ring polymers, *J. Phys.*, 1986, **47**, 2121.
11 T. Sakaue, Ring polymers in melts and solutions: scaling and crossover, *Phys. Rev. Lett.*, 2011, **106**, 167802.
12 S. Obukhov, A. Johner, J. Baschnagel, H. Meyer and J. P. Wittmer, Melt of polymer rings: the decorated loop model, *Europhys. Lett.*, 2014, **105**, 48005.
13 A. Y. Grosberg, Annealed lattice animal model and Flory theory for the melt of non-concatenated rings: towards the physics of crumpling, *Soft Matter*, 2014, **10**, 560.
14 T. Ge, S. Panyukov and M. Rubinstein, Self-similar conformations and dynamics in entangled melts and solutions of non-concatenated ring polymers, *Macromolecules*, 2016, **49**, 708.
15 R. Everaers, A. Y. Grosberg, M. Rubinstein and A. Rosa, Flory theory of randomly branched polymers, *Soft Matter*, 2017, **13**, 1223.
16 J. D. Halverson, G. S. Grest, A. Y. Grosberg and K. Kremer, Rheology of ring polymer melts: from linear contaminants to ring-linear blends, *Phys. Rev. Lett.*, 2012, **108**, 038301.
17 J. D. Halverson, J. Smrek, K. Kremer and A. Y. Grosberg, From a melt of rings to chromosome territories: the role of topological constraints in genome folding, *Rep. Prog. Phys.*, 2014, **77**, 022601.
18 A. Y. Grosberg, S. K. Nechaev and E. I. Shakhnovich, The role of topological constraints in the kinetics of collapse of macromolecules, *J. Phys.*, 1988, **49**, 2095.
19 A. Y. Grosberg, Y. Rabin, S. Havlin and A. Neer, Crumpled globule model of the three-dimensional structure of DNA, *Europhys. Lett.*, 1993, **23**, 373.
20 E. Lieberman-Aiden, N. L. van Berkum, L. Williams, M. Imakaev and T. Ragoczy, *et al.*, Comprehensive mapping of long-range interactions reveals folding principles of the human genome, *Science*, 2009, **326**, 289.
21 L. Mirny, The fractal globule as a model of chromatin architecture in the cell, *Chromosome Res.*, 2011, **19**, 37.
22 A. Rosa and R. Everaers, Structure and dynamics of interphase chromosomes, *PLoS Comput. Biol.*, 2008, **4**, e1000153.
23 M. Barbieri, M. Chotalia, J. Fraser, L.-M. Lavitas, J. Dostie, A. Pombo and M. Nicodemi, Complexity of chromatin folding is captured by the strings and binders switch model, *Proc. Natl. Acad. Sci. U. S. A.*, 2012, **109**, 16173.
24 G. Fudenberg, M. Imakaev, C. Lyu, A. Goloborodko, N. Abdennur and L. A. Mirny, Formation of chromosomal domains by loop extrusion, *Cell Rep.*, 2016, **15**, 2038.
25 A. Goloborodko, J. F. Marko and L. A. Mirny, Chromosome compaction by loop extrusion, *Biophys. J.*, 2016, **110**, 2162.
26 J. Shin, A. G. Cherstvy and R. Metzler, Mixing and segregation of ring polymers: spatial confinement and molecular crowding effects, *New J. Phys.*, 2014, **16**, 5.
27 B. B. Mandelbrot and J. W. Van Ness, Fractional Brownian motions, fractional noises and applications, *SIAM Rev.*, 1968, **10**, 422.
28 M. Imakaev, K. Tchourine, S. Nechaev and L. Mirny, Effects of topological constraints on globular polymers, *Soft Matter*, 2015, **11**, 665.
29 M. V. Tamm, L. I. Nazarov, A. A. Gavrilov and A. V. Chertovich, Anomalous diffusion in fractal globules, *Phys. Rev. Lett.*, 2015, **114**, 178102.
30 S. F. Burlatskii and G. S. Oshanin, Probability distribution for trajectories of a polymer chain segment, *Theor. Math. Phys.*, 1988, **75**, 659.
31 R. M. Gray, Toeplitz and circulant matrices: a review, *Found. Trends Commun. Inf. Theory*, 2006, **2**, 3.

32 R. Kubo, The fluctuation-dissipation theorem, *Rep. Prog. Phys.*, 1966, **29**, 1.

33 P. Hanggi, P. Talkner and M. Borkovec, Reaction-rate theory: fifty years after Kramers, *Rev. Mod. Phys.*, 1990, **62**, 251.

34 W. Deng and E. Barkai, Ergodic properties of fractional Brownian-Langevin motion, *Phys. Rev. E: Stat., Nonlinear, Soft Matter Phys.*, 2009, **79**, 1.

35 I. Bahar, A. R. Atilgan and B. Erman, Direct evaluation of thermal fluctuations in proteins using a single-parameter harmonic potential, *Folding Des.*, 1997, **2**, 173.

36 T. Haliloglu, I. Bahar and B. Erman, Gaussian dynamics of folded proteins, *Phys. Rev. Lett.*, 1997, **79**, 3090.

37 W. Min, G. Luo, B. J. Chrayil, S. C. Kou and X. S. Xie, Observation of a power-law memory kernel for fluctuations within a single protein molecule, *Phys. Rev. Lett.*, 2005, **94**, 198302.

38 M. Dolgushev, J. P. Wittmer, A. Johner, O. Benzerara, H. Meyer and J. Baschnagel, Marginally compact hyperbranched polymer trees, *Soft Matter*, 2017, **13**, 2499.

39 M. Dolgushev, A. L. Hauber, P. Pelagejcev and J. P. Wittmer, Marginally compact fractal trees with semiflexibility, *Phys. Rev. E*, 2017, **96**, 012501.

40 S. Burlatsky, Growth rate of a percolating cluster, *Sov. Phys. JETP*, 1985, **89**, 974.

41 A. Amitai and D. Holcman, Polymer model with long-range interactions: analysis and applications to the chromatin structure, *Phys. Rev. E: Stat., Nonlinear, Soft Matter Phys.*, 2013, **88**, 052604.

42 K. E. Polovnikov, M. Gherardi, M. Cosentino-Lagomarsino and M. V. Tamm, Fractal folding and medium viscoelasticity contribute jointly to chromosome dynamics, *Phys. Rev. Lett.*, 2018, **120**, 088101.

43 D. Jost, P. Carrivain, G. Cavalli and C. Vaillant, Modeling epigenome folding: formation and dynamics of topologically associated chromatin domains, *Nucleic Acids Res.*, 2014, **42**, 9553.

44 L. I. Nazarov, M. V. Tamm, V. A. Avetisov and S. K. Nechaev, A statistical model of intra-chromosome contact maps, *Soft Matter*, 2015, **11**, 1019.

45 S. V. Ulianov, E. E. Khrameeva, A. A. Gavrilov, I. M. Flyamer and P. Kos, *et al.*, Active chromatin and transcription play a key role in chromosome partitioning into topologically associating domains, *Genome Res.*, 2016, **26**, 70.

46 I. S. Reed, P. C. Lee and T.-K. Truong, Spectral representation of fractional Brownian motion in n dimensions and its properties, *IEEE Trans. Inf. Theory*, 1995, **41**, 1439.

47 D. G. Tsalikis, T. Koukoulas, V. G. Mavrantzas, R. Pasquino and D. Vlassopoulos, *et al.*, Microscopic structure, conformation, and dynamics of ring and linear poly(ethylene oxide) melts from detailed atomistic molecular dynamics simulations: dependence on chain length and direct comparison with experimental data, *Macromolecules*, 2017, **50**, 6.

48 J. D. Halverson, W. B. Lee, G. S. Grest, A. Y. Grosberg and K. Kremer, Molecular dynamics simulation study of nonconcatenated ring polymers in a melt. II. Dynamics, *J. Chem. Phys.*, 2011, **134**, 20.

49 M. V. Tamm and K. E. Polovnikov, Dynamics of polymers: classical results and recent developments, *Order, disorder and criticality: advanced problems of phase transition theory*, World Scientific, Singapore, 2018, vol. 5.

50 S. C. Weber, J. A. Theriot and A. J. Spakowitz, Subdiffusive motion of a polymer composed of subdiffusive monomers, *Phys. Rev. E: Stat., Nonlinear, Soft Matter Phys.*, 2010, **82**, 011913.

51 T. J. Lampo, A. S. Kennard and A. J. Spakowitz, Physical modeling of dynamic coupling between chromosomal loci, *Biophys. J.*, 2016, **110**, 338.

52 A. Javer, Z. Long, E. Nugent, M. Grisi and K. Siriwatwetchakul, *et al.*, Short-time movement of *E. coli* chromosomal loci depends on coordinate and subcellular localization, *Nat. Commun.*, 2013, **4**, 3003.

53 D. Michieletto, D. Marenduzzo, E. Orlandini, G. P. Alexander and M. S. Turner, Threading dynamics of ring polymers in a gel, *ACS Macro Lett.*, 2014, **3**, 3.

54 E. Lee, S. Kim and Y. Jung, Slowing down of ring polymer diffusion caused by inter-ring threading, *Macromol. Rapid Commun.*, 2015, **36**, 11.

55 D. G. Tsalikis, V. G. Mavrantzas and D. Vlassopoulos, Analysis of slow modes in ring polymers: threading of rings controls long-time relaxation, *ACS Macro Lett.*, 2016, **5**, 6.

56 The authors of ref. 47 claim that there is a very large (up to 70%) discrepancy between the value of $\sigma^2(s)$ obtained as a best fit of (41) and the value of $\sigma^2(s)$ measured directly from analysing the ring conformations. We have made a similar comparison for the data from ref. 28 and 29 and have found a much smaller discrepancy of 10–20%. This discrepancy deserves some further investigation, such as direct detailed comparison of the raw data of ref. 28, 29 and 47 or some additional computer simulations of the polymer ring melts. However, such an investigation goes beyond the scope of this paper.